Diagnostic Function of 3D Optical Coherence Tomography Images in Diagnosis of Vogt-Koyanagi-Harada Disease at Acute Uveitis Stage

Authors' Contribution:		
Study Design A	ABCDEFG	**Gui-ling Zhao**
Data Collection B	BCDEF	**Rui-zhuang Li**
Statistical Analysis C	BCDE	**Yan-hua Pang**
Data Interpretation D	BCDF	**Xiu-qin Wang**
Manuscript Preparation E	BDF	**Hong-juan Peng**
Literature Search F	BCF	**Jin-fen Wei**
Funds Collection G	CF	**Zhou Zhou**

Department of Ophthalmology, Affiliated Hospital of Guangdong Medical University, Zhanjiang, Guangdong, P.R. China

Corresponding Author: Gui-ling Zhao, e-mail: zhaoguiling@hainan.net
Source of support: Departmental sources

Background: This study analyzed the macular 3D-OCT images of Vogt-Koyanagi-Harada disease (VKH) in uveitis, explored the characteristics of 3D-OCT images of the macular region of VKH, and assessed which characteristics contribute most to VKH diagnosis.

Material/Methods: The 3D-OCT examination of 25 cases of VKH was performed on the macular area, and the image characteristics were analyzed.

Results: Our study included a total of 50 eyes from 25 cases of VKH patients, 10 males and 15 females, aged 17 to 64 years, mean (39.44±11.60) years old. According to OCT B-scan images, 49 (98%) eyes had ERD, 49 (98%) eyes had nerve retinal edema, 36 (72%) eyes had endometrium-like structure (including cysts), 5 (10%) eyes had RPE folds, 35 (70%) eyes had changes in the internal septum, 49 (98%) eyes had RPE monolayer structure outside the ERD region. In ILM-RPE thickness, 49 (98%) eyes had retinal irregular thickening and 31 (62%) eyes had radial stripe changes. In ILM contour figure, 50 eyes (100%) showed exceptional uplift, 5 (10%) eyes had small focal uplift for PED on the RPE surface, and 48 (96%) eyes had wavy ups and downs.

Conclusions: In OCT B-scan imaging, the ERT, retinal edema of the retina, and the RPE monolayer structure outside the range are most likely to occur in VKH. The ILM-RPE thickness chart in 3D reconstruction showed irregular thickening of the retina. The ILM contour graph showed abnormal uplift, and RPE surface wavy ups and downs in VKH most likely to occur.

MeSH Keywords: Imaging, Three-Dimensional • Tomography, Optical Coherence • Uveomeningoencephalitic Syndrome

Full-text PDF: https://www.medscimonit.com/abstract/index/idArt/905931

📄 2871   ⊞ 1   📊 4   📚 33

Background

Vogt-Koyanagi-Harada disease (VKH) is an uncommon multi-system inflammatory disorder characterized by panuveitis with serous retinal detachment [1]. VKH is often associated with neurologic and cutaneous manifestations, including headache, hearing loss, vitiligo, and poliosis. There are 4 clinical stages of VKH: prodromal, acute uveitic, chronic, and recurrent [2]. Most patients seek medical care at the Department of Ophthalmology at the acute uveitic stage when blurred vision becomes a problem. At this stage, the patients may suffer from bilateral blurred vision, first occurring to one eye and then the other several days later. Clinical examinations usually reveal choroidal thickening and protrusion around the optic papilla, with multiple serous retinal detachment, and edema and congestion of optic papilla [3]. There may be pathological changes of retinal pigment epithelium (RPE) associated with multifocal choroiditis. As inflammation affects the protomerite, flare and anterior chamber cells appear. Inflammatory infiltration of the ciliary body and choroid membrane can cause forward shifting of the lens-iris diaphragm, and hence the acute elevation of intraocular pressure or choroidal detachment [4].

Fundus fluorescein angiography (FFA) is an important tool for the diagnosis, follow-up, and prognostic prediction of VKH [5]. Inflammation can lead to delayed perfusion of posterior pole choroid, which manifests as a spot-like filling defect or choroid delay in its early stage [6]. Later, there will be dotted leakage, diffusion, and merging of fluorescein in the RPE layer, indicating multiple detachment of neural epithelium. Late-stage VKH manifests comma-shaped hyper-fluorescence upon FFA [7–9].

Optical coherence tomography (OCT) is a new imaging diagnostic method [10]. It has the advantages of non-invasiveness, high safety, high resolution (5 μm axial resolution), fast scanning speed, and large data acquisition capability (which allows for 3D reconstruction and stratified analysis). Independent from the influence of ocular aberration and pupil diameter, this technique requires no reference plane and has a high repeatability. OCT is considered an ideal method for quantitative analysis of internal retina structure. Researchers have previously described OCT manifestations of VKH at the acute uveitic stage [11,12]. However, those manifestations included a number of limitations.

In the present study, we analyzed cross-sectional (B-scans) and 3D images of macula using 3D-OCT, and present new findings on OCT manifestations of VKH at the acute uveitic stage.

Material and methods

Subjects

We included VKH patients who were treated at the outpatient clinic or hospitalized from January 2013 to December 2016. Specifically, according to the diagnostic criteria given by Read et al. [13], the first onset cases of bilateral or unilateral blurred vision, bilateral diffuse chorioiditis or chorioretinopathy, shallow detachment of neural epithelium or exudative retinal detachment, confirmed by FFA or B-scan ultrasonography, were included. Those who did not cooperate with examination or had corneal or lenticular opacity were excluded. The following were also excluded: patients with high myopia or blurred vision caused by other conditions, incomplete or less accurate data, a history of trauma or eye surgeries, and patients with atypical clinical manifestations or uncertain diagnosis.

General examinations

Routine eye examinations, slip lamp tests, fundus examinations, and non-contact tonometry were performed. FFA, eye B-ultrasonography, and other eye or systemic examinations were performed if necessary.

Macular OCT

The Topcon 3D OCT-1000 Optical Coherence Tomographer was used to detect ocular structures at a wavelength of 840 nm. Axial and lateral resolutions were set to 5 μm and 20 μm, respectively. Scans were made at a speed of 18 000 A/s, a depth of 2.0 mm, and a range of 6×6 mm.

Pupils were diluted naturally or using drugs in sitting position. Examinations were conducted in a dark room. With the mandible on the jaw bracket, the patients were told to stare at the fixation lamp inside or outside the lens. Macular thickness was analyzed in 3D macular mode. Acquisition time was approximately 5 s. The parameter values were calculated automatically using 3D OCT-1000 from the scanned data.

We analyzed 64 horizontal B-scan images and retinal thickness maps (ILM-RPE). Different intensities of light signals and retinal thicknesses were represented in OCT images on a rainbow color scale. In the B-scan images, tissue color indicated reflection intensity. The following colors represented reflected light intensity in decreasing order: white, red, orange, green, blue, and black. Black indicted the tissue with the weakest light reflection (Figure 1).

Retinal thickness was determined from the distance from the internal limiting membrane (ILM) to the RPE. The ILM-RPE maps were generated within a range of 6×6 mm in the center of the
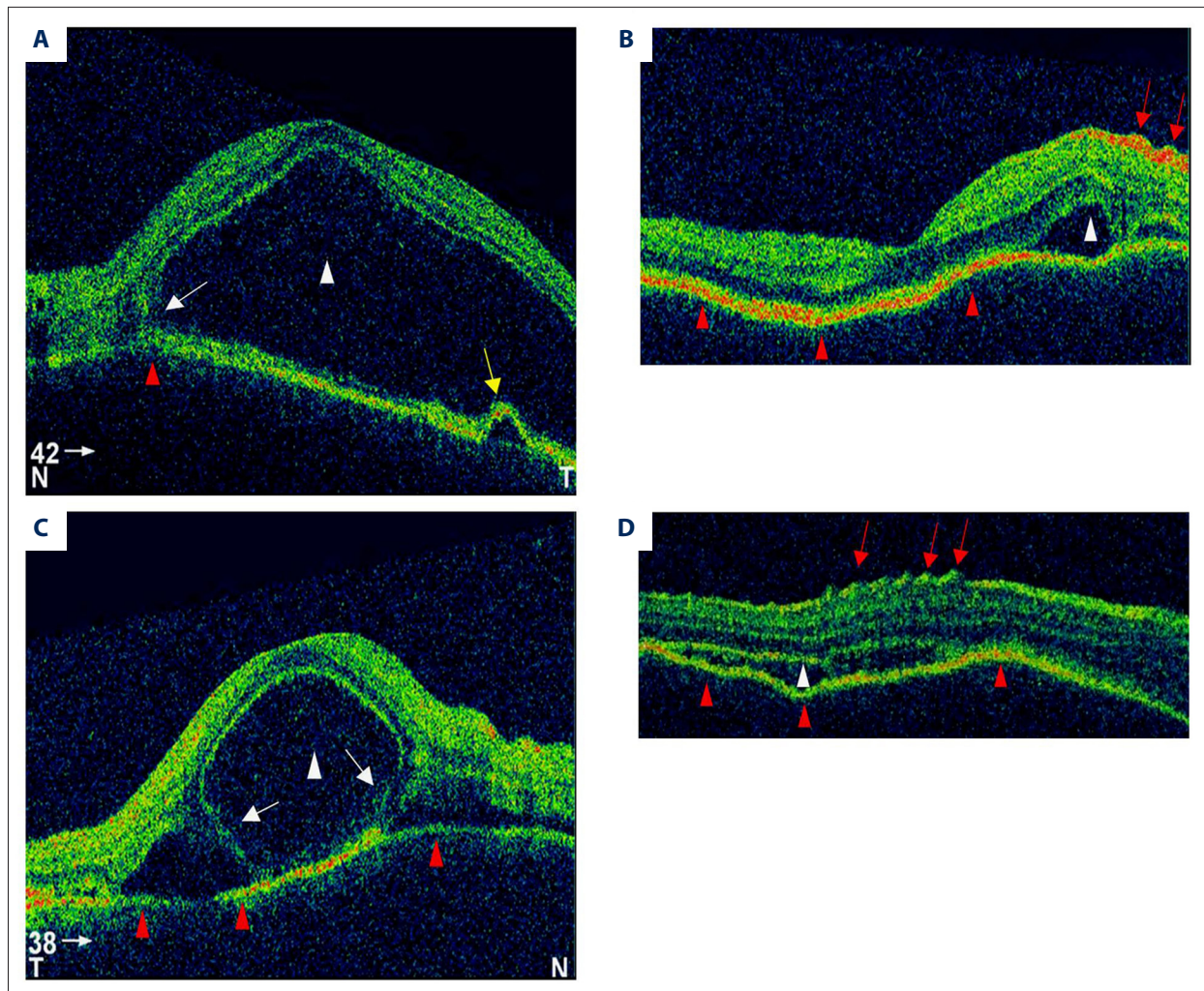
Figure 1. B-scan image of VKH. (**A**) Exudative retinal detachment (ERD) (indicated by the white arrowheads), with the inclusion angle between the left side of the detached region and pigment epithelium not sharp (white arrow); focal Pigment epithelium detachment (PED) (yellow arrow) on the right side; significant fluctuation of pigment epithelium (red arrow). (**B**) ERD in nasal retina (white arrowhead), with FI (fluctuation in the internal limiting membrane) (red arrows), replacement of double-layer structure of pigment epithelium by monolayer and fluctuation (red arrowheads). (**C**) ERD (white arrowhead), with stripes or MS in the detached region (white arrows), and fluctuation in pigment epithelium (red arrowheads). (**D**) ERD (white arrowhead), with thickening photoreceptor cells; replacement of double-layer structure of pigment epithelium by monolayer, fluctuation in pigment epithelium (red arrowheads), and FI (red arrow).

retina. Thickness was represented by pseudocolors, with white corresponding to the greatest thickness. Red, orange, yellow, green, and blue indicated successively decreasing levels of thickness. ILM contour maps and RPE surface maps were reconstructed with using computer software (Figure 1).

Definition of symptoms

Exudative retinal detachment (ERD) was defined as the complete or near-complete separation of the retinal neuro-epithelium from the pigment epithelium. Membrane structure (MS) was defined as the spot-like, linear, or membranous light reflection of the detached region. Pigment epithelium detachment (PED) was the separation of the RPE from Bruch's membrane or the choroid membrane. Upon OCT, PED manifested as a dome-shaped protrusion of RPE towards the retina, usually with a uniform area of low reflection behind it. The RPE fold (RF) was the loss of the smooth surface of the RPE layer, resulting in various forms of protrusion. One peak or trough in the RPE layer was defined as an RF. The loss of the smooth surface of the ILM layer, resulting in fluctuating changes, was considered a fluctuation in the internal limiting membrane (FI). As defined by Lin et al. [14], FI was fluctuation with at least 2 peaks or troughs in the ILM layer. Thinning of RPE was the
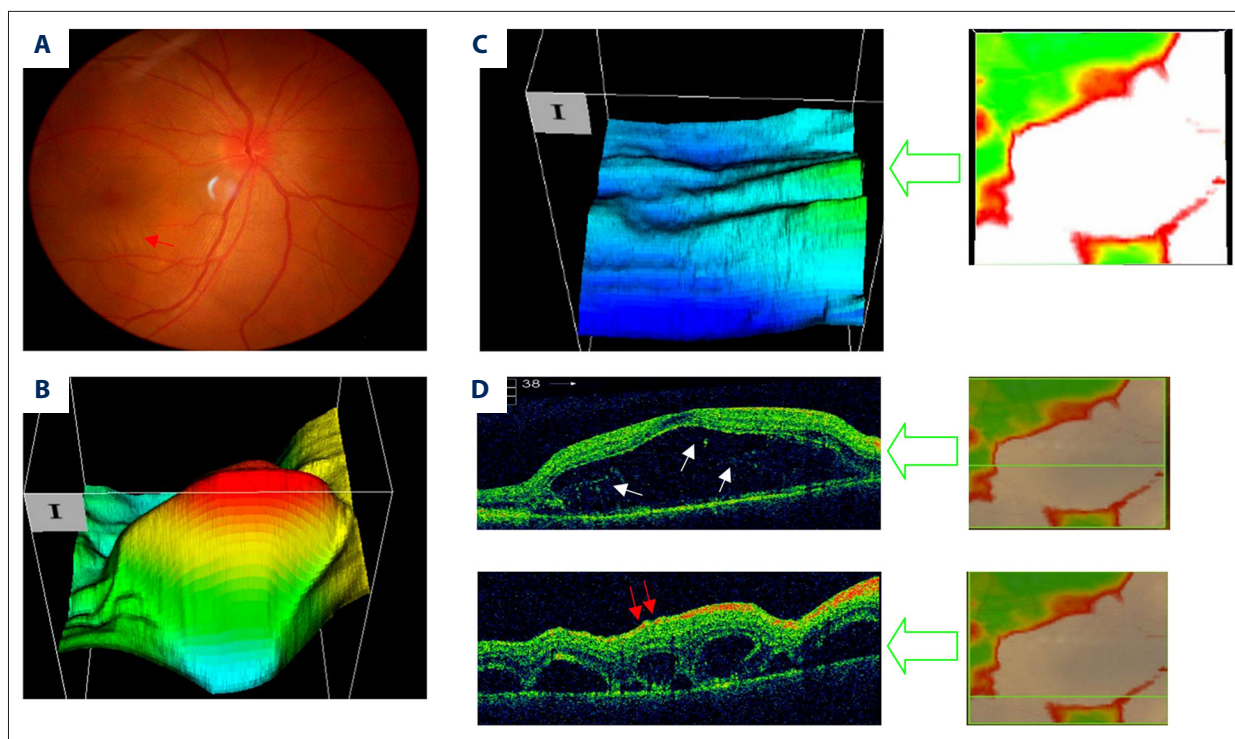
Figure 2. Right eye of patient # 8 with vision acuity FC/30 cm. (**A**) This image is a color image displaying neuro-epithelium protrusions in the macula and RF below the macula (red arrow). (**B**) This image is the ILM topography map demonstrating the major peak in the center surrounded by irregular protrusions. (**C**) This image is the ILM-RPE map of the right eye. White indicates irregular regions formed by several merging protrusions. (**D**) The upper image is an RPE topography map showing fluctuations in the vertical direction, which indicate X. The lower images are B-scan images of the positions indicated by the blue line in the right lower image. The upper image shows ERD with spot-like MS in the detached region, the disappearance of the RPE double-layer structure, and weakening reflection, without the apparent folds. The lower image is a merged image of the detached regions in the neuro-epithelium. FI (red arrow).

disappearance of the 3-layer structure of pigment epithelium outside ERD, with weakening of light reflection (Figure 1).

The 3D views included the ILM-RPE map, ILM contour, and RPE surface. White or red areas on the ILM-RPE map were considered to be thickened (Figure 2). Observation of radial stripes indicated pathological changes in a radial pattern (Figure 3). The 2 observations may occur alone or in combination. Abnormalities on the ILM contour maps were defined as the disappearance of normal macular structure, with local protrusions or recesses. Abnormality on the RPF surface map was defined as small protrusions (PED) (Figure 4) or wavy fluctuations (Figures 2, 3).

Results

Baseline information

Twenty-five VKH patients with 50 eyes were included (10 males, 15 females, aged 17 to 64 years old, with an average age of 39.44±11.60 years). They sought medical care at our hospital at 1 to 40 days (average 8.96±9.31 days) after onset. None of them had received hormone therapy before. Twenty-three cases were affected in bilateral eyes, and 1 case was affected in only one eye; another case was affected first in one eye and then the other. The vision acuity ranged from hand movement to 1.0, with intraocular pressure ≤21 mmHg. No abnormalities were found in the anterior segments in 48 eyes of 24 cases. Mixed congestion was found in 2 eyes for 1 case, with dust-like deposit KP (+) and aqueous flare (+).

Fundus examination

Fundus examination revealed optic disc congestion in 32 eyes (64%), 1 or more dome-shaped protrusions were found in the posterior poles of 49 eyes (98%), and radial stripes were observed in 40 eyes (80%).

B-scan images of macula

ERD was observed in 49 eyes (98%) using B-scan images. MS (including septa) was found in 36 eyes (72%), PED was found
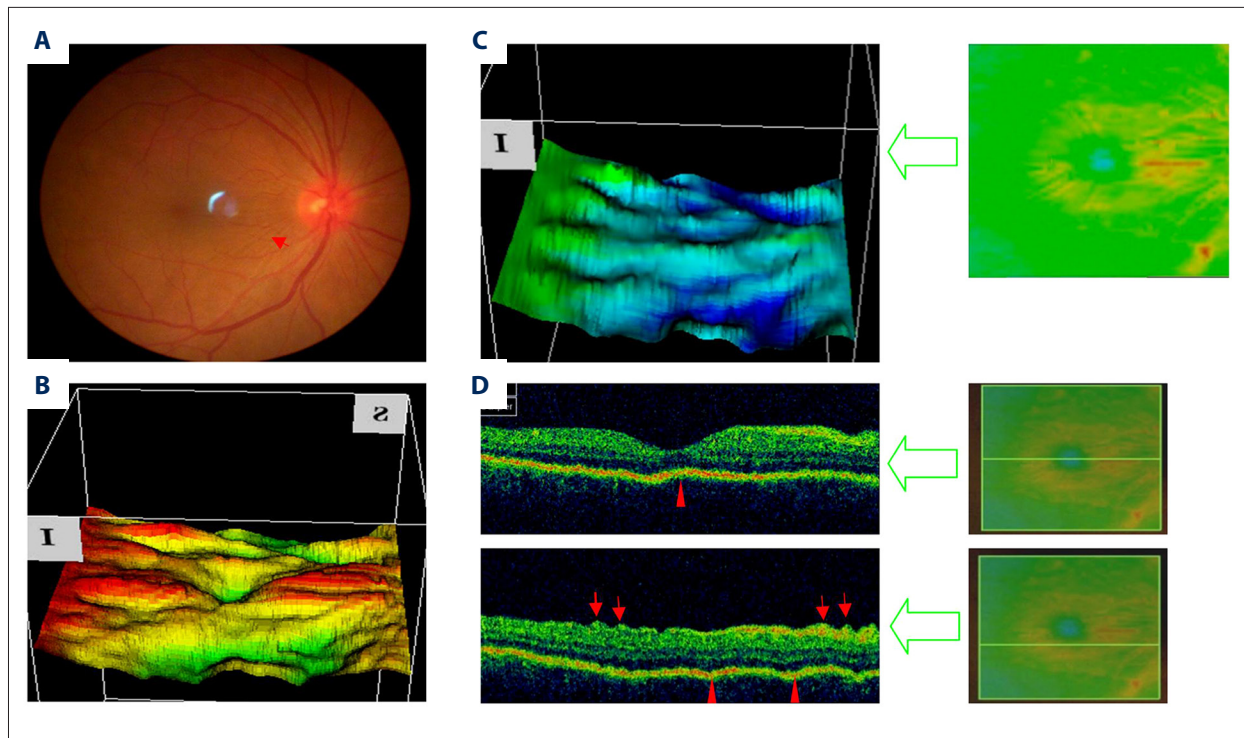
Figure 3. Right eye of patient #2 with a visual acuity of 0.25. (**A**) This image displays a color image of the RF (red arrow). (**B**) This ILM contour map and middle upper RPE surface maps reveal the uneven surface of the retina. The right upper ILM-RPE thickness map (**C**) indicates stripes in the nasal part of the optic disc and around the macula. (**D**) The B-scan images of the positions indicated by the green lines in the right lower image. The upper one shows the central fovea of macula, with the disappearance of the 3-layer RPE structure and the appearance of mild folds (red arrowhead). The lower half of the panel shows FI (red arrow), with the disappearance of the 3-layer RPE structure and the appearance of mild folds (red arrowheads)

in 5 eyes (10%), RF was identified in 30 eyes (60%), FI was found in 35 eyes (70%), and RPE thinning was discovered in 49 eyes (98%).

3D images of macula

On ILM-RPE thickness maps, irregular thickening indicated by white or red colors was found in 48 eyes (98%), and radial stripes were found in 31 eyes (62%). All cases had abnormal protrusion on ILM contour maps. On RPE surface maps, 5 eyes (10%) exhibited small protrusions diagnosed as PED; 48 eyes (96%) displayed wavy fluctuations (Table 1).

Discussion

Extensive choroidal inflammation and exudative retinal detachment (ERD) are the major fundus manifestations of VKH at the acute uveitic stage [15,16]. Starting from the choroid, the lesion soon affects the retina, leading to ERD in some positions; even the non-detached regions may show inflammatory response.

ERD is the most common clinical manifestation of VKH. Zhao et al. [16] reported ERD in all 18 cases. Attia et al. [17] presented a report of 18 cases with VKH, half of which had ERD. By analyzing B-scan images of the VKH cases, we found ERD in 98% of affected eyes. Upon OCT, ERD associated with VKH usually manifests as detachment of neuro-epithelium with varying degrees of MS in the detached regions [18,19]. Yamaguchi et al. [19] analyzed OCT manifestations of ERD and proposed the division of ERD into true serous RD and retinal effusion. The former is associated with distinct layers of the detached retina. The inclusion angle between the detached retina and pigment epithelium is sharp. The space below the retina is optically clear without spot-like, linear, or membranous hyper-reflection. Retinal effusion is similar to serous RD except for a thin layer of residual retina on the surface of RPE. There are spot-like, linear, or membranous hyper-reflections in the detached regions, and the cysts are separated by septa. Compared to true serous RD, retinal effusion usually predicts more severe and extensive leakage of pigment epithelium, as well as more severe choroidal inflammation. This division was supported by Tsujikawa et al. [20] and Lee et al. [21]. It was pointed out by Lee et al. [21] that retinal effusion might be related to inflammation and swelling of photoreceptor
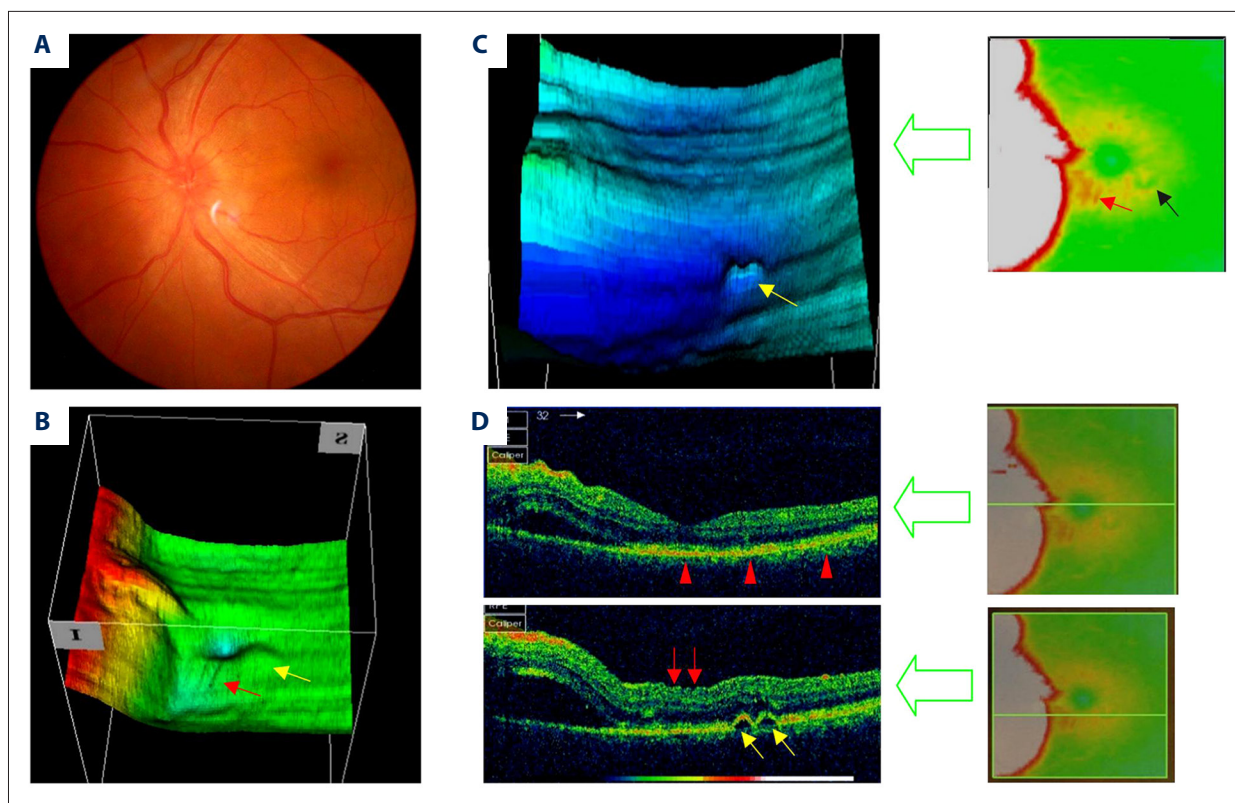
691

Indexed in: [Current Contents/Clinical Medicine] [SCI Expanded] [ISI Alerting System] [ISI Journals Master List] [Index Medicus/MEDLINE] [EMBASE/Excerpta Medica] [Chemical Abstracts/CAS]

Figure 4. Left eye of patient # 8 with vision acuity of 0.6. (**A**) This is a color image of the eye. An obscure boundary and congestion of the optic disc, but no ERD nor radial stripes, were observed. (**B**) This image is an ILM contour map showing the protrusion (red) into the nasal side, a small subtemporal protrusion into the macula (yellow arrow), and 2 vertical stripes directly below the macula on the nasal side (red arrow). (**C**) This image is an RPE surface map, which shows considerable fluctuation in RPE on the nasal side, as well as a small focal protrusion corresponding to the subtemporal protrusion on the ILM contour map (yellow arrow). Corresponding to the ILM protrusion and small focal protrusion in RPE, the top right panel shows thinned regions indicated by 2 small patches of green in the subtemporal region (black arrow). There are radial stripes in the macula, and 2 vertical stripes directly below the macula on the nasal side (red arrow); they correspond to the stripes in the ILM contour map. (**D**) These are the B-scan images of the positions indicated by green lines in the right lower image. The upper image shows the central fovea of macula, with an FI on the nasal side (red arrow). ERD is observed, with uneven light reflection from the 3-layer structure of the non-detached region in RPE, indicating an obscure structure (red arrow). The lower one shows ERD in the nasal side, with focal PED on the right side (yellow arrow) and FI in the center (red arrow).

cells. According to Yamaguchi et al. [19], MS was the exudative membrane caused by inflammatory response at the acute stage of VKH. The membrane accumulating below the retinal neuro-epithelium is rich in proteins and cellulose. After the fibrin is dissolved by glucocorticoids, the membrane is degraded into particle-like structure. It is also believed that MS will disappear rapidly after hormone therapy. Zhao et al. [16] also considered MS to be the leakage below the retina due to retinal inflammation. Lin et al. [14] suggested the use of pathological examination to determine whether MS is part of the retinal neuro-epithelium or other inflammatory substances.

Lin et al. [14] proposed FI and defined it as the observation of at least 2 peaks or troughs in the ILM layer. FI was very common in our study. It occurred in 70% of cases. Lin et al. [14] inferred that at the acute stage of VKH, cytokines mediated by

inflammatory cells in RPE or ciliary body might lead to pathological changes in retinal morphology. Fluctuation of ILM, the innermost layer of the retina, may be among the major pathological retinal changes caused by acute-stage inflammatory response. Sensitivity and specificity of this feature in diagnosis of VKH was 55.0% and 100.0%, respectively. Therefore, we speculated that this feature was capable of differentiating between central serous retinopathy and VKH, which would also be verified in future study.

Normal RPE is shown as a 3-layer structure on OCT. The IS/OS layer or the innermost layer, is separated from the other 2 layers at the central fovea of macula. In other regions, the 3 layers cling closely together [22]. However, RPE is separated from the inflamed photoreceptor outer segments in ERD, and light reflection only occurs in the remaining monolayer of RPE.

Table 1. Demographic data and clinical features of patients with acute Vogt-Koyanagi-Harada disease.

No.	Age (yr)	Sex	BCV (R/L)	Duration (d)	Fundus manifestations		
					RD (R/L)	Radial folds (R/L)	PED (R/L)
1	34	M	0.06/0.06	3	+/+	+/+	–/–
2	55	M	0.25/0.05	30	–/+	+/+	+/+
3	49	F	0.2/0.06	10	+/+	+/+	+/+
4	53	F	0.1/0.15	4	+/+	+/+	+/+
5	30	F	0.1/0.2	6	+/+	+/+	–/–
6	47	F	0.4/0.4	7	+/+	+/+	+/+
7	45	F	0.15/0.15	2	+/+	+/+	–/–
8	43	M	FC/0.6	3	+/+	+/–	+/+
9	40	F	0.2/0.06	40	+/+	+/+	+/+
10	39	F	0.3/0.2	1	+/+	–/–	–/–
11	45	M	0.2/0.12	4	+/+	–/–	+/+
12	33	M	0.08/0.3	10	+/+	+/+	–/–
13	28	F	0.04/0.05	5	+/+	+/+	+/+
14	53	F	0.05/0.05	10	+/+	+/+	–/–
15	17	F	0.6/0.1	3	+/+	+/+	–/–
16	64	M	0.15/0.15	7	+/+	–/–	+/+
17	47	M	0.04/0.04	5	+/+	+/+	+/+
18	41	F	0.2/HM	20	+/+	+/+	–/–
19	20	F	0.05/0.1	7	+/+	+/–	+/+
20	24	F	0.15/0.15	7	+/+	+/+	+/+
21	50	F	0.12/0.1	4	+/+	+/–	+/+
22	33	M	0.25/0.4	1	+/+	+/–	+/+
23	33	F	0.15/0.05	20	+/+	+/+	–/–
24	31	M	FC/FC	10	+/+	+/+	+/+
25	32	M	0.25/1.0	5	+/+	+/+	+/+
Total (%)					49 (98%)	40 (80%)	32 (64%)

Table 1 continued. Demographic data and clinical features of patients with acute Vogt-Koyanagi-Harada disease.

No.	SD OCT					
	RD (R/L)	Subretinal septa (R/L)	thinning of RPE (R/L)	PED (R/L)	Folds of RPE (R/L)	Fluctuation of ILM (R/L)
1	+/+	+/+	+/+	–/–	+/+	–/–
2	+/–	–/–	+/+	–/–	+/+	+/+
3	+/+	–/–	+/+	–/–	+/+	+/+
4	+/+	+/+	+/+	–/–	+/+	+/+
5	+/+	+/–	+/+	–/–	+/+	+/+
6	+/+	–/–	+/+	–/–	+/+	+/+
7	+/+	+/+	+/+	–/–	+/+	–/–
8	+/+	+/–	+/+	+/+	–/–	+/+
9	+/+	+/+	+/+	–/–	+/+	–/–
10	+/+	+/+	+/+	+/+	+/+	–/–
11	+/+	+/–	+/+	–/–	+/–	+/+
12	+/+	+/–	+/+	–/–	+/+	–/–
13	+/+	+/–	+/+	–/–	–/–	+/+
14	+/+	+/+	+/+	–/–	+/+	+/+
15	+/+	+/+	+/+	+/–	–/–	+/–
16	+/+	+/+	+/+	–/–	–/–	–/+
17	+/+	+/+	+/+	–/–	+/–	+/+
18	+/+	+/+	+/+	–/–	+/–	+/+
19	+/+	+/+	+/+	–/–	–/–	+/–
20	+/+	+/+	+/+	–/–	–/–	+/+
21	+/+	+/+	+/+	–/–	+/+	+/–
22	+/+	+/+	+/+	–/–	–/–	–/+
23	+/+	+/+	+/+	–/–	+/+	+/+
24	+/+	+/–	+/+	–/–	–/+	+/+
25	+/+	–/–	+/–	–/–	–/–	+/+
Total (%)	49 (98%)	36 (72%)	49 (98%)	5 (10%)	30 (60%)	35 (70%)

Table 1 continued. Demographic data and clinical features of patients with acute Vogt-Koyanagi-Harada disease.

No.	ILM-RPE thickness map		Abnormal protrusion of ILM contour	Wavy fluctuation of RPE surface
	Irregular protrusion (R/L)	Radial stripes (R/L)		
1	+/+	–/–	+/+	+/+
2	+/–	+/+	+/+	+/+
3	+/+	+/+	+/+	+/+
4	+/+	+/+	+/+	+/+
5	+/+	+/+	+/+	+/+
6	+/+	+/+	+/+	+/+
7	+/+	–/–	+/+	+/+
8	+/+	–/+	+/+	+/+
9	+/+	–/–	+/+	+/+
10	+/+	–/–	+/+	+/+
11	+/+	+/+	+/+	+/+
12	+/+	+/+	+/+	+/+
13	+/+	+/+	+/+	+/+
14	+/+	–/+	+/+	+/+
15	+/+	+/–	+/+	+/+
16	+/+	–/+	+/+	+/+
17	+/+	–/+	+/+	+/+
18	+/+	+/+	+/+	+/+
19	+/+	+/–	+/+	+/+
20	+/+	–/+	+/+	+/+
21	+/+	–/–	+/+	+/+
22	+/+	–/–	+/+	+/+
23	+/+	+/+	+/+	+/+
24	+/+	+/+	+/+	+/+
25	+/–	+/+	+/+	–/–
Total (%)	48 (96%)	31 (62%)	50 (100%)	48 (96%)

We observed RPE beyond the detached region of neuro-epithelium in VKH and often observed an absence of the 3-layer structure, with weakening light reflection. Among our cases, VKH originated from choroidal inflammation, which later affected RPE and retinal neuro-epithelium. If inflammation affected RPE, the 3-layer structure of RPE would disappear upon OCT. This feature can be used to differentiate between VKH and RD due to non-inflammatory causes.

Pigment epithelium detachment (PED) is the separation of the RPE from Bruch's membrane or choroid membrane. Upon OCT, PED usually manifests as dome-shaped RPE protrusions stretching towards the retina, usually with a uniform low reflection area behind it [23]. Some reports have mentioned this feature in VKH [14,19]. We identified typical PED in 5 eyes. Although PED is not an uncommon condition, a few cases with PED might not have been discovered due to limited scan range.

RPE fold is the loss of smooth surface of RPE and manifests as protrusion of RPE. Kato et al. [24] defined RPE fold as the observation of at least 2 peaks or troughs. Considerable fluctuations were observed in many RPE folds in this study; thus, we defined RPE fold as the observation of at least 1 peak or trough. According to this criterion, 30 eyes had RPE folds, accounting for 60% of cases. This is in line with findings from similar studies, including 71.4% in Kato et al.'s study [24] and 52% in Wu et al.'s study [25].

The incidence of RPE folds was reported to be 63.6% by Attia et al. [17]. To analyze RPE folds, Gupta et al. [26] used 3D mode, which allowed for a full observation of RPE. We also used the 3D mode, which revealed RPF folds in 96% of the cases. This proportion was much higher than those found using B-scan, which suggests that the 3D mode is more accurate in detecting lesions. As to the causes of RPE folds, Hosoda et al. [27] performed EDI-OCT and put forward the concept of RPE undulation index, which correlated to choroidal thickness. Moreover, they suggested the inflammation and edema of choroid were the causes of RPE folds in VKH and that uneven thickening of choroid led to uneven RPE protrusions. Kato et al. [24] did not observe RPE folds in individuals with or without uveitis in non-VKH cases. Thus, RPE folds can be used as a diagnostic criterion for VKH.

ILM-RPE elevation map is a representation of the results of 3D OCT, which are obtained by the computer automatically calculating the distance from ILM to RPE and generating the topography. Thickness is represented by pseudocolors on a rainbow color scale. For normal retina, the diameter of central fovea of macular is about 1 mm and is represented by green color. The macula is the thickest at 1 to 3 mm. There is a transition from green to yellow color, which represents the circular protrusion, with thinning towards the periphery, which is

represented as the transition from yellow to green with scattered bluish-green [28]. We found abnormal thickening on the ILM-RPE elevation map in 96% of the eyes with VKH, which manifested as the connection between white and red. These changes were in accordance with the dome-shaped protrusion caused by ERD and were also related to edema and thickening of the non-detached retina. The ILM-RPE map shows the thickness distribution of the entire retina represented by salient pseudocolors, so the lesions can be easily discovered from the ILM-RPE map.

Radial stripes were detected in 31 eyes (62%) from the ILM-RPE elevation maps. These stripes have not been explicitly reported before. The 3D images provided by Wu et al. [25] contained these stripes, but no more details were given about the stripes other than the thickening. We further analyzed the fundus images of VKH cases and found as many as 80% of the cases had radial stripes. Although the significance of the radial stripes was not mentioned, they can be clearly visualized from the images [1,29]. We found correlations between radial stripes on the elevation map and those on the color images of the fundus. The changes were consistent with FI (Figure 4). We considered this to be different manifestations of the same symptom upon different examinations.

Actually, previous studies [30–33] have also reported the same topic of diagnostic role of optical coherence tomography in acute Vogt-Koyanagi-Harada. However, the present study is different from the previously published articles. Our study proved the diagnostic values of optical coherence tomography in different respects. We found that according to the OCT B-scan images, the ERT, retinal edema of the retina, and the PRE monolayer structure outside the range are most likely to occur in VKH, and the ILM contour graph showed that abnormal uplift and RPE surface wavy ups and downs in VKH were most likely to occur, which disagrees with previously published articles. Some of the indexes and the experiments used in these studies were valuable and significant; therefore, we plan to use some of these valuable methods from those articles to improve our subsequent research.

Although our study found some interesting results, it has certain limitations. We did not investigate the role of OCT in differentiating VKH from the other causes of inflammatory panuveitis, such as sarcoidosis, Behcet's disease, and sympathetic ophthalmia. Other factors, such as history and extraocular manifestations, are very helpful in differentiating these from each other. Therefore, we plan to investigate the role of OCT in differentiating VKH from other causes of inflammatory panuveitis.

Conclusions

In OCT B-scan images, the ERT, retinal edema of the retina, and the RPE monolayer structure outside the range are most likely to occur in VKH. The ILM-RPE thickness chart in 3D reconstruction showed irregular thickening of the retina. The ILM contour graph showed abnormal uplift, and RPE surface wavy ups and downs in VKH were most likely to occur.

Conflict of interests

None.

References:

1. Burkholder BM: Vogt-Koyanagi-Harada disease. Curr Opin Ophthalmol, 2015; 26(6): 506–11

2. Sakata VM, da Silva FT, Hirata CE et al: Diagnosis and classification of Vogt-Koyanagi-Harada disease. Autoimmun Rev, 2014; 13(4–5): 550–55

3. Shinohara K, Moriyama M, Shimada N et al: Analysis of shape of eyes and structure of optic nerves in eyes with tilted disc syndrome by swept-source optical coherence tomography and three-dimensional magnetic resonance imaging. Eye (Lond), 2013; 27(11): 1233–41

4. Fu J, Sun F, Liu W et al: Subconjunctival delivery of Dorzolamide-Loaded poly microparticles produces sustained lowering of intraocular pressure in rabbits. Mol Pharm, 2016; 13(9): 2987–95

5. Banerjee PJ, Davies NP: An innocuous adverse effect of routine fundus fluorescein angiography. JAMA Ophthalmol, 2016; 134(1): e153624

6. Xu J, Gao X, Yang C et al: Resolvin D1 attenuates MPP+ induced Parkinson disease via inhibiting inflammation in PC12 cells. Med Sci Monit, 2017; 23(1): 2684–91

7. Arellanes-Garcia L, Hernandez-Barrios M, Fromow-Guerra J et al: Fluorescein fundus angiographic findings in Vogt-Koyanagi-Harada syndrome. Int Ophthalmol, 2007; 27(2–3): 155–61

8. Jap A, Chee SP: Imaging in the diagnosis and management of Vogt-Koyanagi-Harada disease. Int Ophthalmol Clin, 2012; 52(4): 163–72

9. Chee SP, Jap A, Cheung CM: The prognostic value of angiography in Vogt-Koyanagi-Harada disease. Am J Ophthalmol, 2010; 150(6): 888–93

10. Ma X, Chen Y, Liu X et al: Effect of refractive correction error on retinal fiber layer thickness: A spectralis optical coherence tomography study. Med Sci Monit, 2016; 22(1): 5181–89

11. Parc C, Guenoun JM, Dhote R et al: Optical coherence tomography in the acute and chronic phases of Vogt-Koyanagi-Harada disease. Ocul Immunol Inflamm, 2005; 13(2–3): 225–27

12. Okamoto Y, Miyake Y, Horio N et al: Delayed regeneration of foveal cone photopigments in Vogt-Koyanagi-Harada disease at the convalescent stage. Invest Ophthalmol Vis Sci, 2004; 45(1): 318–22

13. Read RW, Holland GN, Rao NA et al: Revised diagnostic criteria for Vogt-Koyanagi-Harada disease: Report of an international committee on nomenclature. Am J Ophthalmol, 2001; 131(5): 647–52

14. Lin D, Chen W, Zhang G et al: Comparison of the optical coherence tomographic characters between acute Vogt-Koyanagi-Harada disease and acute central serous chorioretinopathy. BMC Ophthalmol, 2014; 14(1): 87

15. Morita C, Sakata VM, Rodriguez EE et al: Fundus autofluorescence as a marker of disease severity in Vogt-Koyanagi-Harada disease. Acta Ophthalmol, 2016; 94(8): e820–21

16. Zhao C, Zhang MF, Dong FT et al: Spectral domain optical coherence tomography of Vogt-Koyanagi-Harada disease: Novel findings and new insights into the pathogenesis. Chin Med Sci J, 2012; 27(1): 29–34

17. Attia S, Khochtali S, Kahloun R et al: Clinical and multimodal imaging characteristics of acute Vogt-Koyanagi-Harada disease unassociated with clinically evident exudative retinal detachment. Int Ophthalmol, 2016; 36(1): 37–44

18. Ishihara K, Hangai M, Kita M et al: Acute Vogt-Koyanagi-Harada disease in enhanced spectral-domain optical coherence tomography. Ophthalmology, 2009; 116(9): 1799–807

19. Yamaguchi Y, Otani T, Kishi S: Tomographic features of serous retinal detachment with multilobular dye pooling in acute Vogt-Koyanagi-Harada disease. Am J Ophthalmol, 2007; 144(2): 260–65

20. Tsujikawa A, Yamashiro K, Yamamoto K et al: Retinal cystoid spaces in acute Vogt-Koyanagi-Harada syndrome. Am J Ophthalmol, 2005; 139: 670–77

21. Lee JE, Park SW, Lee JK et al: Edema of the photoreceptor layer in Vogt-Koyanagi-Harada disease observed using high-resolution optical coherence tomography. Korean J Ophthalmol, 2009; 23(2): 74–79

22. Shi F, Chen X, Zhao H et al: Automated 3-D retinal layer segmentation of macular optical coherence tomography images with serous pigment epithelial detachments. IEEE Trans Med Imaging, 2015; 34(2): 441–52

23. Bloom SM, Singal IP: The outer Bruch membrane layer: A previously undescribed spectral-domain optical coherence tomography finding. Retina, 2011; 31(2): 316–23

24. Kato Y, Yamamoto Y, Tabuchi H et al: Retinal pigment epithelium folds as a diagnostic finding of Vogt-Koyanagi-Harada disease. Jpn J Ophthalmol, 2013; 57(1): 90–94

25. Wu W, Wen F, Huang S et al: Choroidal folds in Vogt-Koyanagi-Harada disease. Am J Ophthalmol, 2007; 143(5): 900–1

26. Gupta V, Gupta A, Gupta P et al: Spectral-domain cirrus optical coherence tomography of choroidal striations seen in the acute stage of Vogt-Koyanagi-Harada disease. Am J Ophthalmol, 2009; 147(1): 148–53

27. Hosoda Y, Uji A, Hangai M et al: Relationship between retinal lesions and inward choroidal bulging in Vogt-Koyanagi-Harada disease. Am J Ophthalmol, 2014; 157(5): 1056–63

28. Hitzenberger C, Trost P, Lo PW et al: Three-dimensional imaging of the human retina by high-speed optical coherence tomography. Opt Express, 2003; 11(21): 2753–61

29. Hou S, Liao D, Zhang J et al: Genetic variations of IL 17F and IL 23A show associations with Behcet's disease and Vogt-Koyanagi-Harada syndrome. Ophthalmology, 2015; 122(3): 518–23

30. Aggarwal K, Agarwal A, Mahajan S et al: The role of optical coherence tomography angiography in the diagnosis and management of acute Vogt-Koyanagi-Harada disease. Ocul Immunol Inflamm, 2016; 20(1): 1–12

31. Liu XY, Peng XY, Wang S et al: Featuers of optical coherence tomography for the diagnosis of Vogt-Koyanagi-Harada disease. Retina, 2016; 36(11): 2116–23

32. Aggarwal K, Agarwal A, Deokar A et al: Distinguishing features of acute Vogt-Koyanagi-Harada disease and acute central serous chorioretinopathy on optical coherence tomography angiography and en face optical coherence tomography imaging. J Ophthalmic Inflamm Infect, 2017; 7(1): 3

33. Chee SP, Chan SN, Jap A: Comparison of enhanced depth imaging and swept source optical coherence tomography in assessment of choroidal thickness in Vogt-Koyanagi-Harada disease. Ocul Immunol Inflamm, 2016; 12(1): 1–5